

# Finite Element Modelling of Atomic Force Microscope Cantilever beams with Uncertainty in Material and Dimensional Parameters

Bin WANG<sup>1)</sup>, Xiao WU<sup>2)</sup>, Tat-Hean GAN<sup>1)</sup>, Alexis RUSINEK<sup>3)</sup>

<sup>1)</sup> *School of Engineering and Design, Brunel University*  
UK  
e-mail: bin.wang@brunel.ac.uk

<sup>2)</sup> *School of Mechanical Engineering, Southwest Jiaotong University*  
P. R. China  
e-mail: wuxiaobs@163.com

<sup>3)</sup> *National Engineering School of Metz ENIM*  
*Laboratory of Mechanics, Biomechanics, Polymers and Structures – LaBPS, EA 4632*  
1 route d’Ars Laquenexy, CS 65820 57078 METZ Cedex 3, France  
e-mail: rusinek@enim.fr

The stiffness and the natural frequencies of a rectangular and a V-shaped micro-cantilever beams used in Atomic Force Microscope (AFM) were analysed using the Finite Element (FE) method. A determinate analysis in the material and dimensional parameters was first carried out to compare with published analytical and experimental results. Uncertainties in the beams’ parameters such as the material properties and dimensions due to the fabrication process were then modelled using a statistic FE analysis. It is found that for the rectangular micro-beam, a  $\pm 5\%$  change in the value of the parameters could result in 3 to 8-folds (up to more than 45%) errors in the stiffness or the 1st natural frequency of the cantilever. Such big uncertainties need to be considered in the design and calibration of AFM to ensure the measurement accuracy at the micron and nano scales. In addition, a sensitivity analysis was carried out for the influence of the studied parameters. The finding provides useful guidelines on the design of micro-cantilevers used in the AFM technology.

**Key words:** atomic force microscope, cantilever, stiffness, natural frequency, sensitivity analysis.

## 1. INTRODUCTION

Atomic Force Microscopes (AFMs) have been widely used for scanning measurement at the micron and nano scales. A micro-cantilever with a sharp probe at its free end is a key component of an AFM, as shown in Fig. 1. It works in

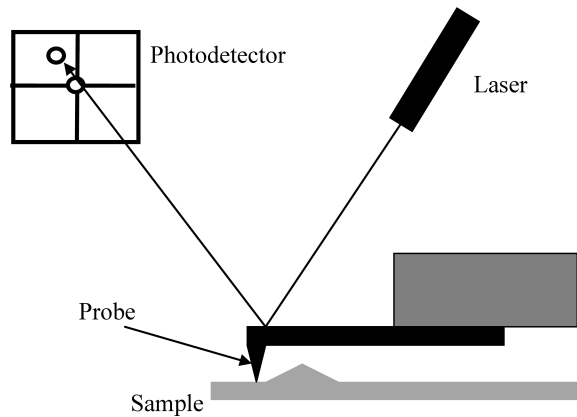


FIG. 1. The working principle of an AFM.

a way similar to a gramophone stylus. While the probe scans a surface of a sample, the contact force between the probe tip and the surface being scanned leads to a small elastic deflection of the micro-cantilever. The deflection is measured by reflecting a laser beam to a position-sensitive photodetector which records the movement of the reflected laser beam. By converting the signal generated from the photodetector, a topographic image of the scanned surface can be generated.

The quality of the image obtained from an AFM is greatly dependent on knowing the elastic parameters of the cantilever. Depending on the mode of application, either the bending stiffness or the 1st natural (resonant) frequency of the cantilever is used. A good knowledge of these, often referred to as the calibration of the cantilever, is of fundamental importance to both the manufacturer and the user as it determines the accuracy of the measurement. Since the invention of AFM, the study of the calibration of AFM cantilevers has been an essential subject in the development of the technology [1].

An AFM can be used in different modes of measurement, such as contact, noncontact and tapping modes [1–3]. The classification is based on the type of the interaction between the probe tip and the surface being scanned. For the contact mode, the probe touches the sample surface all the time. It is customary to call this type of measurement as the static mode. As a high magnitude contact force may damage the sample surface, a cantilever of a lower stiffness is preferred. A flexible cantilever will also yield in large deformation, leading to higher measurement sensitivity.

An AFM can also be used in a non-contact and tapping manner as termed the dynamic mode. In the dynamic mode, the cantilever is externally oscillated at or close to its 1st natural frequency about 5 to 10 nano-meter above the sample surface such that the probe only comes in contact with the sample once

in each vibration cycle. Changes in the frequency due to the contacts provide information of the sample surface profile. In this mode, a higher stiffness, or higher natural frequencies, normally only the 1st one being used for resonance response, would give more accurate results.

There exist a variety of shapes for AFM cantilevers which are used in different modes for different applications. The most commonly used ones are the rectangular and the V-shaped configurations, as shown in Fig. 2.

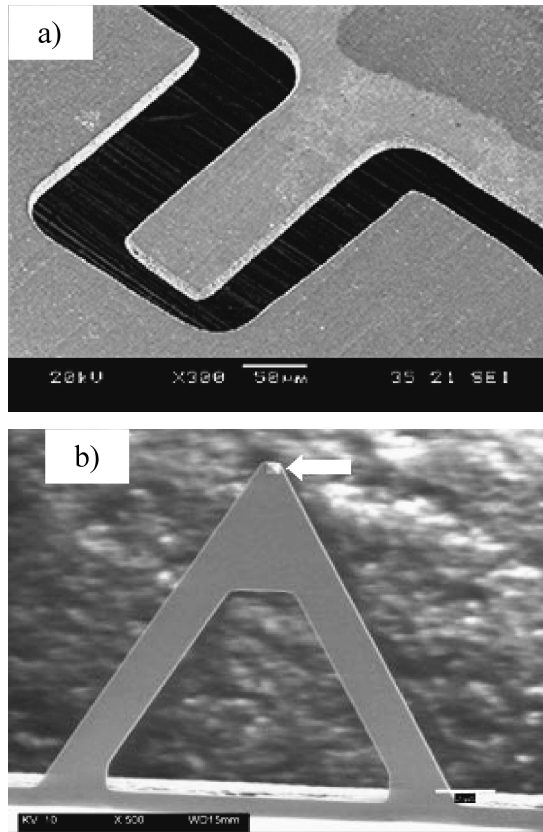


FIG. 2. SEM (Scanning electron microscope) images of (a) a rectangular cantilever and (b) a V-shaped cantilever. The arrow in (b) indicates the probe tip. A better view of the tip is shown in Fig. 6.

AFM cantilevers are mostly made of silicon and silicon nitride in a micro-electronic fabrication process. Cantilevers are made by first patterning a circular silicon dioxide dot on a silicon wafer. Silicon beneath the silicon dioxide dot is then etched, undercut and oxidized. Subsequently, the silicon post becomes a tip after the removal of the oxide. Then, the cantilever is formed by etching the boron doped silicon [1, 2].

The micro-fabrication process, however, often leads to variable stoichiometry of the cantilevers, which causes difficulties in controlling the dimensions of the cantilever, such as the thickness and the length, as well as in ensuring the value of the material properties, such as the Young's modulus and the density. All these will cause variation in the stiffness and the natural frequencies of fabricated cantilevers [4].

To obtain the value of the stiffness and the natural frequencies of the cantilever, both experimental and analytical approaches have been proposed. For the measurement of the stiffness, the cantilever is pushed at the free end by a force of a known magnitude and the corresponding deflection is measured, from which the stiffness can be calculated based on the classic elastic beam theory. The known force can be produced in different ways. One way is to attach a tungsten sphere [5] of a known mass as shown in Fig. 3. Another commonly seen method is to use a reference cantilever of known stiffness to press against the unknown one. From the deflection of the known cantilever, the interaction force can be determined. This force is then used together with the deflection of the unknown cantilever to determine its stiffness. Such static methods can achieve an accuracy of 2–5% [6].

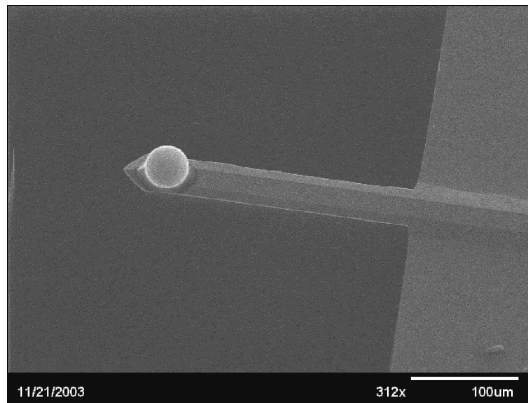


FIG. 3. A cantilever with a tungsten sphere glued to its free end [8].

The stiffness can also be determined by dynamic test methods which rely on the determination of the natural frequencies of the cantilever. One method is to fix a mass [7] to the free end then monitoring the change in the natural frequency of vibration. This technique is applicable to any cantilevers. However, as the mass has to be permanently added (to sustain with the vibration) it is destructive and the error in measurement is relatively large [9, 10].

Apart from experimental measurements, analytical modelling has also been used to derive theoretical values of the stiffness and the natural frequencies based on the classic structural mechanics. For V-shaped cantilevers, different

formulae have been proposed, eg. BUTT *et al.* [12], SADER and WHITE [13] and SADER *et al.* [14]. One of the examples is the Parallel Beam Approximation (PBA) by ALBRECHT *et al.* [11] in which the V shape is approximated by two rectangles in parallel. Analytical modelling requires accurate knowledge of the cantilever properties, such as the Young's modulus and the geometry, with the latter usually measured from scanning electron micrograph (SEM).

The structural geometry parameters of a rectangular and a V-shaped cantilever are shown in Fig. 4, with notations indicating the dimensional parameters needed in determining the mechanical performance of the cantilever.

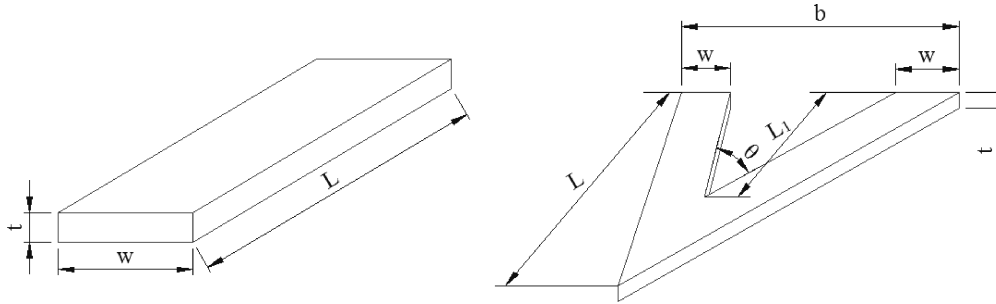


FIG. 4. Geometric parameters of the rectangular and V-shaped cantilevers (the probe tip at the free end is ignored as negligible in affecting the mechanical performance).

AFM cantilevers are typically very thin and SEM measurement accuracy error can be of 3%. This may lead to errors in calculation as the thickness is of 3rd power in beam deflection formula. In addition, material constants such as the Young's modulus may also vary due to the anisotropic deposit of the thin film, to a variation range typically more than 3% [13].

In this work, we are motivated to use the finite element (FE) method as an alternative approach to obtain the stiffness and the natural frequencies of an AFM cantilever, and to introduce a range of randomness to the numerical model to examine the influence of the uncertainties in the material and dimensional parameters of the cantilever. The FE model will also allow a sensitivity study to be carried out to determine the significance of the parameters involved.

Both the dynamic and static FE models were built for a rectangular and V-shaped cantilever, respectively. The paper is organised in the following order. First a deterministic FE analysis is discussed to verify the FE outcomes with published theoretical and experimental results. Then the variation in the beam dimensions and the Young's Modulus are introduced, assuming a uniform random distribution in the values of the parameters such as the geometric and the Young's modulus between  $\pm 5\%$  of their nominal values. Finally a sensitivity analysis was carried out to obtain the influential effect of the parameters on the stiffness and the 1st natural frequency of the cantilever.

## 2. FINITE ELEMENT ANALYSIS

A commercial finite element code ANSYS (Ansys Inc.) was used to model the micro-cantilevers. The nominal values of the parameters used in the simulations were obtained from a manufacturer of the cantilevers, for instance, AC-160 tapping mode rectangular cantilever shown in Figs. 5 and 6 by Olympus

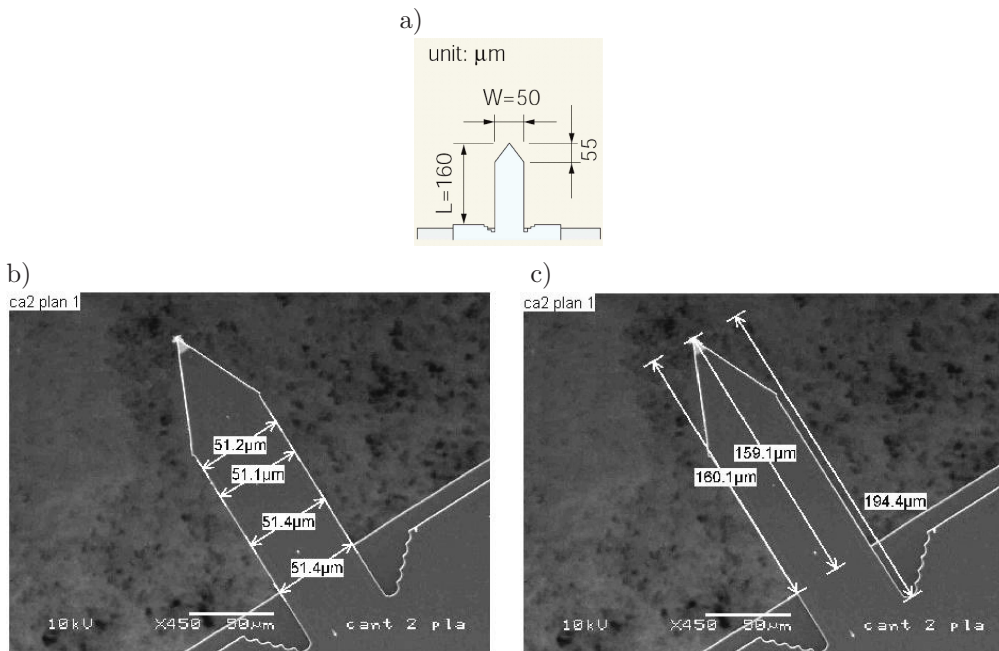


FIG. 5. (a) The manufacturer's dimensions of the AC-160 micro cantilever [16], (b) and (c) SEM images of plane view dimensions [8].

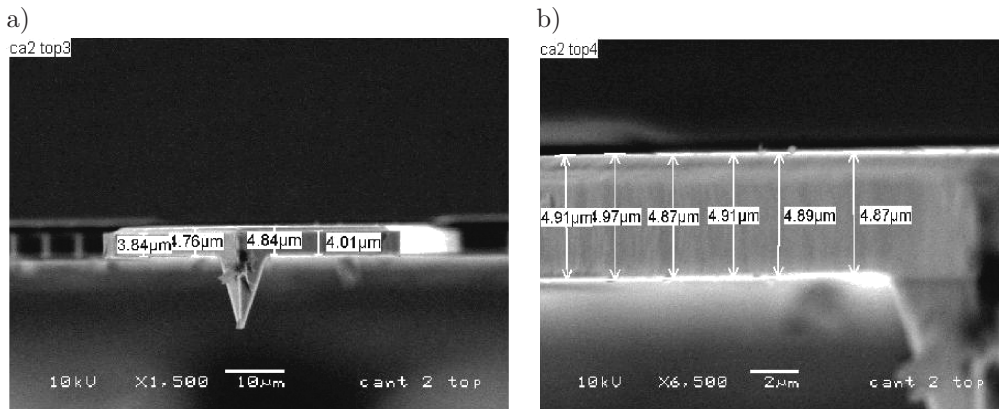


FIG. 6. SEM images of the thickness of the cantilever [8], a) view in the axial direction at the free end, b) close-up side view of the cantilever root.

Corporation [16]. These include both the dimensions and the material properties, as listed in Table 1.

**Table 1.** Inputs of the FE model for the rectangular cantilever.

Parameters	Nominal value	Min. value (−5%)	Max. value (+5%)
Length $L$ [ $\mu\text{m}$ ]	160	152	168
Width $W$ [ $\mu\text{m}$ ]	50	47.5	52.5
Thickness $t$ [ $\mu\text{m}$ ]	4.6	4.37	4.83
Young's Modulus $E$ [GPa]	167.4	159.0	175.8
Density $\rho$ [ $\text{kg}/\mu\text{m}^3$ ]	$2.33 \times 10^{-15}$		
Poisson's ratio $\nu$	0.27		

Measurements of the physical dimensions were also performed using SEM [8]. The average length and width are  $159.6 \mu\text{m}$  and  $51.28 \mu\text{m}$ , respectively, with the uncertainty relative to the nominal value being less than 1%. The thickness of the cantilever is critical for bending deflection, and the uncertainty was found to be much higher. Compared to the nominal value of  $4.6 \mu\text{m}$ , the measured thickness varies from  $3.84$  to  $4.97 \mu\text{m}$  (corresponding error  $-6.5\%$  and  $8\%$ ), respectively. In the FE model, an average thickness of  $4.88 \mu\text{m}$  was used based on SEM measurement.

The value of the Young's modulus, density, Poisson's ratio and geometric parameters used in the FE analysis are listed in Table 1 for the rectangular configuration and Table 2 for the V-shaped one. To cater for the variation in the parameters, a randomness of uniform distribution in dimensions and the Young's modulus were introduced in a range of  $\pm 5\%$  of the corresponding nominal values. The density and Poisson ratio were assumed constant due to lack of available data. The nominal values of the parameters (either the average of the measure-

**Table 2.** Inputs of the FE model for the V-shaped cantilever.

Parameters	Nominal value	Min. value (−5%)	Max. value (+5%)
Length $L$ [ $\mu\text{m}$ ]	190	180.5	199.5
Length $L_1$ [ $\mu\text{m}$ ]	87.5	83.125	91.875
Width $b$ [ $\mu\text{m}$ ]	165	156.75	173.25
Single limb width $w$ [ $\mu\text{m}$ ]	33.3	31.635	34.965
Thickness $t$ [ $\mu\text{m}$ ]	0.6	0.57	0.63
Young's Modulus $E$ [GPa]	179.0	170.1	188.0
Density $\rho$ [ $\text{kg}/\mu\text{m}^3$ ]	$2.33 \times 10^{-15}$		
Poisson's ratio $\nu$	0.27		

ment, or the value provided by the manufacturer) were used in a deterministic analysis first to verify the FE model with literature results. The cantilevers were assumed to be isotropic and homogeneous, with one end fully clamped as the boundary condition.

The models were built using a quadrilateral shell element provided by ANSYS. After a convergence test, approximately 27000 elements were used for the rectangular model and 46000 elements for the V-shaped cantilever model. Figure 7 illustrates an example of the output of dynamic analyses of both configurations.

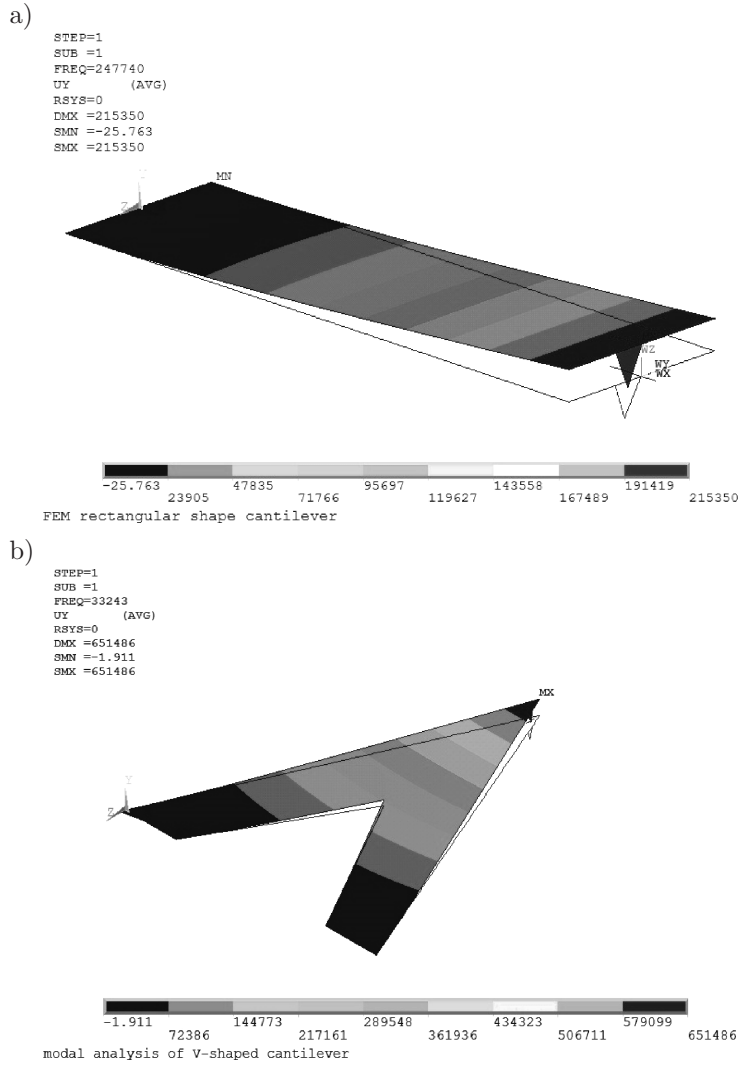


FIG. 7. The first mode of free vibration of: a) the rectangular cantilever and b) the V-shaped cantilever.

### 2.1. Rectangular cantilever

**2.1.1. Dynamic FE modelling for natural frequencies.** For the modal analysis of the rectangular cantilever, the first three modes are shown in Table 3. The nominal frequency values listed in the table indicate the frequencies obtained with the nominal values of the parameters, while the minimum and maximum are the frequencies from the corresponding minimum (95% of the nominal) and maximum (105%) input parameters as listed in Table 1. The percentage values in brackets in Table 3 are the differences to the nominals. It is clearly shown that the ranges of difference from  $-16.1\%$  to  $19.4\%$  are much bigger than the 5% variation in the input parameters.

**Table 3.** First three natural frequencies of the rectangular cantilever.

Mode	Deformation	Natural Frequency [kHz]		
		Nominal	Minimum	Maximum
1st	Flexure	247.74	207.83 ( $-16.1\%$ )	295.73 ( $19.4\%$ )
2nd	Flexure	1546.9	1299.1 ( $-16.0\%$ )	1750.0 ( $13.1\%$ )
3rd	Torsion	1607.7	1480.1 ( $-7.9\%$ )	1845.0 ( $14.8\%$ )

The stiffness  $k$  can be calculated analytically from the first natural frequency

$$(2.1) \quad k = (2\pi f_0)^2 m_e,$$

where  $f_0$  is the first natural frequency of the cantilever vibration. The effective mass  $m_e$  is equal to the multiplication of the cantilever mass  $m$  and a geometrical factor  $n$ .  $n$  is proposed as 0.2427 by SADER *et al.* [9], or 0.25 by CLEVELAND *et al.* [7]. Table 4 shows the value of the stiffness from Eq. (2.1) and the classic beam theory. Again, big variations are shown from  $-16.1\%$  and  $49.2\%$  to the nominal values, corresponding to  $-5\%$  and  $+5\%$  change in the input values, respectively.

**Table 4.** Stiffness obtained from the 1st natural frequency.

		Nominal	Minimum	Maximum
1st natural frequency [kHz]		247.74	207.83 ( $-16.1\%$ )	295.73 ( $19.4\%$ )
Stiffness $k$ [N/m]	Eq. (2.1) with $n = 0.2427$ [9]	50.42	33.63 ( $-33.3\%$ )	75.25 ( $49.2\%$ )
	Eq. (2.1) with $n = 0.25$ [7]	51.94	34.64 ( $-33.3\%$ )	77.52 ( $49.2\%$ )
	Analytical $k = \frac{Et^3w}{4L^3}$	49.73	33.24 ( $-33.2\%$ )	74.02 ( $48.8\%$ )

*2.1.2. Static FE modelling for stiffness.* The static method is an alternative way to calculate the stiffness using deflections under specific loading. In the FE model, a point load of the magnitude of 1 and 10  $\mu\text{N}$  was applied perpendicular to the cantilever at its free end. Table 5 gives the deflection and the stiffness calculated. Note that variations of deflection changes are the opposite sense to those of the stiffness. The two loads produce identical stiffness under elastic deformation.

**Table 5.** FEA results of the stiffness of the rectangular cantilever model.

Load		Nominal	Minimum	Maximum
$F = 1 \mu\text{N}$	Deflection	0.019	0.028 (48.7%)	0.012 (-36.8%)
	Stiffness $K$ [N/m]	53.180	35.759 (-32.8%)	80.302 (51.0%)
$F = 10 \mu\text{N}$	Deflection	0.188	0.280 (48.9%)	0.125 (-33.5%)
	Stiffness $K$ [N/m]	53.180	35.759 (-32.8%)	80.301 (51.0%)

The stiffness is given as 53.18 N/m by the static FEM, 49.73 N/m by the analytical modelling, 50.42 N/m by the dynamic FEM and 42 N/m by the manufacturer, as compared is in Fig. 8. It shows that both FE models and the theoretical method agree well, but with a notable difference (more than 20%) to the value provided by the manufacturer.

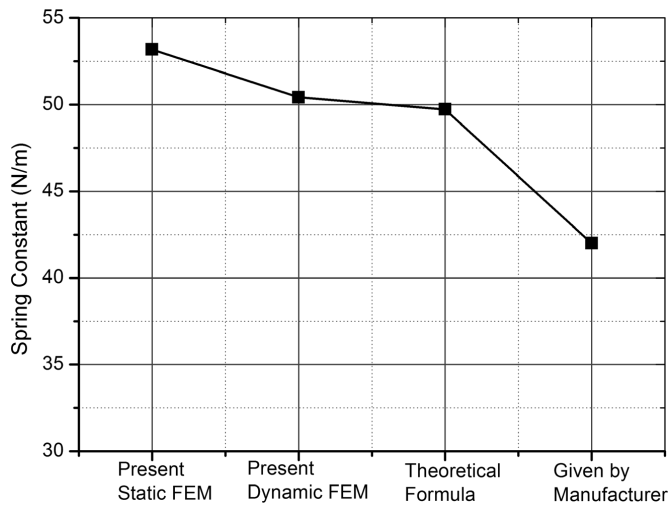


FIG. 8. Comparison of the stiffness of the rectangular cantilever obtained by different methods.

## 2.2. V-shaped cantilevers

For the V-shaped cantilever, a randomness variation of  $\pm 5\%$  was also introduced in the input value of the parameter. Results of the dynamic FEM for the

nominal, minimum and maximum values are shown in Table 6. The “magnified” errors in the natural frequencies are given in brackets.

**Table 6.** The first five natural frequencies of V-shaped cantilevers and differences to the normal value.

Mode	Description	Natural frequency [kHz]		
		Nominal	Minimum	Maximum
1st	Flexure	33.243	26.939 (−19.0%)	41.097 (23.6%)
2nd	Flexure	171.797	141.644 (−17.6%)	208.652 (21.5%)
3rd	Torsion	190.727	157.166 (−17.6%)	231.784 (21.5%)

The first mode is compared with the theoretical result and experimental measurement [5] as given in Table 7, showing an error range within 8% for the 1st mode and 14% for the 2nd.

**Table 7.** Comparison of the 1st natural frequencies from theory, experimental [5] and FEA.

Theoretical [kHz]	Experimental [kHz]	FEM [kHz]
34	31.5	33.2

A static FE analysis was also carried out with  $\pm 5\%$  error introduced to the input value, as shown in Table 8. Like in the realiser results, the increased errors are clearly evidential.

**Table 8.** FEA results of the stiffness under different loads for the V-shaped beam model.

Force		Nominal	Minimum	Maximum
$F = 1 \mu\text{N}$	Deformation	10.289	14.766 (43.5%)	7.198 (−30.0%)
	Stiffness $K$	0.0972	0.068 (−30.0%)	0.139 (43.0%)
$F = 10 \mu\text{N}$	Deformation	102.887	147.659 (43.5%)	71.981 (−30.0%)
	Stiffness $K$	0.0972	0.068 (−30.0%)	0.139 (43.0%)

Results of different theoretical models [12–14], the dynamic FEM, and the static FEM agree well except that of ALBRECHT [11], as shown in Fig. 9.

Results of finite element simulations clearly show an increased error bands in the cantilevers stiffness and natural frequencies due to small variations in the input values of cantilever dimensions and material property. For design and calibration purpose, the “error contribution” of each of the input parameters needs



FIG. 9. Comparison of the stiffness of the V-shaped beam obtained by different methods.

to be investigated. In the following section, a sensitivity study is discussed, aiming to identify the influence of the input parameters on the overall performance of the cantilevers.

### 3. SENSITIVITY STUDY

#### 3.1. Mathematical model for sensitivity analysis

For both the rectangular and V-shaped cantilevers, a 5% variation in the parameter values leads to much bigger changes in the natural frequencies and the stiffness. From the design view point, it is useful to know the scale of influence of each parameter on the performance of the cantilevers. In this section, a sensitivity analysis is presented on the significance of the dimension and material parameters.

Sensitivity to a variable is defined by the first-order derivative of a function with respect to the variable. For instance, for a multivariate function  $f(X)$  with  $X$  representing the variable vector of  $k$  parameters,  $X = (x_1, x_2, \dots, x_k)$ , the sensitivity of function  $f$  to its  $j$ -th parameter  $x_j$  can be expressed as

$$(3.1) \quad S_i = \frac{\partial f(X)}{\partial x_j}, \quad j = 1, 2, \dots, k.$$

A higher magnitude of  $S_j$  indicates a stronger sensitivity of  $f$  to  $x_i$ . Note that  $S_j$  can be both positive and negative for the correlation of  $f$  to  $x_i$ .

In the static analysis, the global governing equations is

$$(3.2) \quad [K]\{\delta\} = \{F\},$$

where  $[K]$  denotes the structure's stiffness matrix,  $\{\delta\}$  the nodal displacement and  $\{F\}$  the external loading.

Taking partial derivatives of Eq. (3.2) and noticing that the external loading  $F$  is independent of the structural and material parameters, thus  $\frac{\partial F}{\partial x_j} = 0$ , we have

$$(3.3) \quad \frac{\partial\{\delta\}}{\partial x_j} = -[K]^{-1} \frac{\partial[K]}{\partial x_j} \{\delta\}.$$

From FEA, the nodal displacement  $\{\delta\}$  can be calculated. Then the displacement sensitivity  $\frac{\partial\{\delta\}}{\partial x_j}$  can then be obtained from equation (3.3).

For the dynamic analysis, the equation of free vibration can be expressed as

$$(3.4) \quad [K] - \lambda_i[M]\{\varphi_i\} = 0, \quad i = 1, 2, \dots, n,$$

where  $[M]$  is the mass matrix;  $\lambda_i$  the  $i$ -th eigenvalue of the natural frequency,  $\{\varphi_i\}$  the  $i$ -th order eigenvectors; and  $n$  the total number of degree of freedom.

Taking partial derivative of Eq. (3.4) with respect to the parameter  $x_j$  yields in

$$(3.5) \quad \left( \frac{\partial[K]}{\partial x_j} - \frac{\partial\lambda_i}{\partial x_j}[M] - \lambda_i \frac{\partial[M]}{\partial x_j} \right) \{\varphi_i\} = 0.$$

Multiplying Eq. (3.5) on the left by  $\{\varphi_i\}^T$  and introducing a generalized mass  $m_i = \{\varphi_i\}^T [M] \{\varphi_i\}$ , the sensitivity of the  $i$ -th order eigenvalue  $\lambda_i$  with respect to the  $j$ -th parameter  $x_j$  is

$$(3.6) \quad \frac{\partial\lambda_i}{\partial x_j} = \frac{\{\varphi_i\}^T \left( \frac{\partial[K]}{\partial x_j} - \lambda_i \frac{\partial[M]}{\partial x_j} \right) \{\varphi_i\}}{m_i}.$$

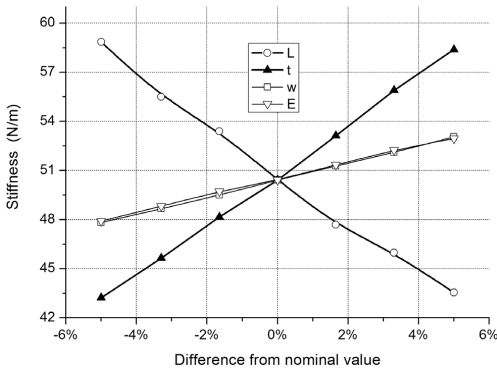
The variation of input parameters in this study was limited within the range from  $-5\%$  to  $+5\%$  of their nominal values and was chosen randomly based on the uniform distribution assumption. After the value of the parameters was randomly chosen, a finite element simulation was carried out. From the FE results, the sensitivity data was calculated from Eqs. (3.3) and (3.6). This is virtually a Monte Carlo approach when dealing with uncertainty in variables.

A commercial code Isight (Dassault Systems Co) was used for the sensitivity study in connection with ANSYS. Isight picks up parameter values based on random sampling for each parameter in a uniform distribution. The chosen values were then used by ANSYS for simulation. The obtained FE results are then used by the Isight again to calculate the partial derivatives to obtain the sensitivity of the stiffness or the 1st natural frequency on individual input parameter.

3.2. Sensitivity analysis results

The effect of the input parameter variables on the stiffness and the first natural frequencies were obtained, as given in Fig. 10, for both the rectangular and V-shaped micro-cantilevers. The notations of the legends are defined in Fig. 4. In Fig. 10, the horizontal axes shows the range of variations of the input parameters, and the vertical axes give the value of the magnitude of the

a) rectangular cantilevers



b) V-shape cantilevers

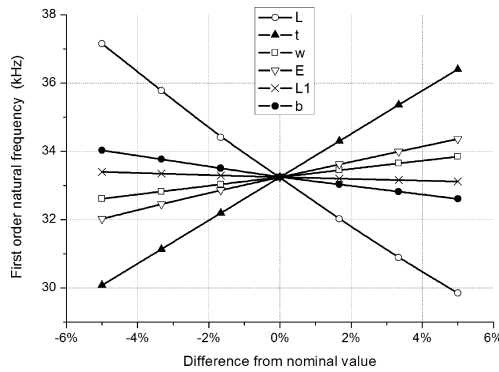
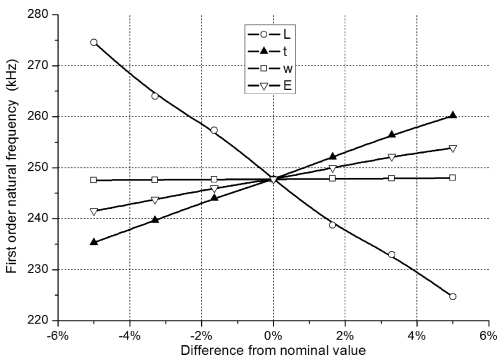
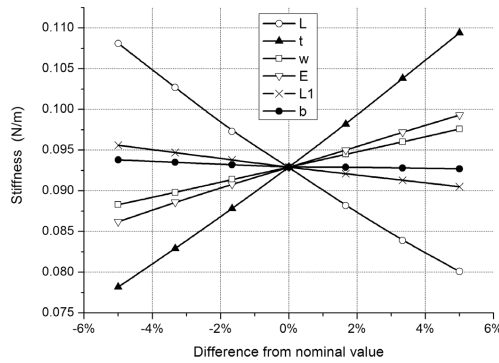


FIG. 10. Effect of input parameters on the stiffness and the 1st natural frequency. Parameter notations are defined in Fig. 4.

stiffness or the 1st natural frequency. The influence appears to be all linear approximately, due to the narrow range of variation.

For the rectangular cantilever in Fig. 10a, the cantilever length  $L$  has the biggest impact overall on both the stiffness and the 1st natural frequency with negative slopes, meaning that an increase in the length will lead to a reduction in the stiffness and the 1st natural frequency (ie. negative correlation). This is expected from the classic beam theory as the flexural behaviour of a cantilever is reversely proportion to the length of a beam. Useful conclusions can be drawn from the figure. For instance, we can see that for every 1% increase in the cantilever's length, the natural frequency is reduced by approximately 5.0 Hz. For every 1% increase in beam thickness, the natural frequency is increased by 2.5 Hz. The values of the slope of these linear relationships in Fig. 10 are given in Table 9 for the significance of the influence of each parameter.

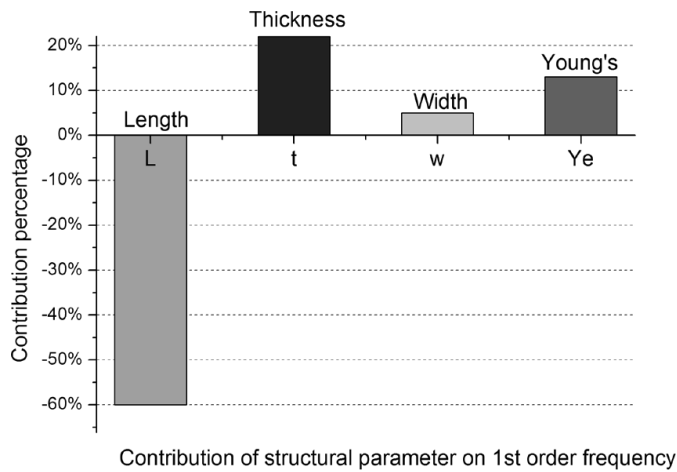
**Table 9.** Variation of the 1st natural frequency and the stiffness to 1% change of each input parameter's nominal value.

		$L$	$t$	$w$	$E$	$L_1$	$b$
Rectangular	1st Natural frequency [kHz]	-4.98	2.49	0.04	1.24		
	Stiffness [N/m]	-1.53	1.52	0.52	0.50		
V-shaped	1st Natural frequency [kHz]	-0.73	0.39	0.12	0.23	-0.03	-0.14
	Stiffness [N/m]	-0.003	0.003	0.001	0.001	-0.001	-0.0001

A pareto diagram is constructed in Fig. 11 to show the contribution of influence of the input parameters to the 1st natural frequency, as against the overall influence (100%) by all parameters. Figure 11a shows that the contribution rate of the length  $L$  is found to be approximately 60%, and in the negative correlation, while the thickness is the next most influential parameter for the rectangular beam.

It is interesting to see that the thickness  $t$  has a much stronger effect for the V-shaped cantilever, as seen in Fig. 11(b), even more than that of the length. Considering the difficulty in controlling the thickness in the fabrication process and in its measurement (in comparison to the length  $L$ ), this should be the parameter of utmost significance for the design, fabrication and calibration of the macro-cantilever in AFM. It is also noted that the Young's modulus has a bigger effect proportionally for the V-shaped cantilever than that for the rectangular one (20% vs. 13%). It shows that different strategies should be adopted in selecting parameters for the design and fabrication of different cantilevers.

a) rectangular cantilevers



b) V-shape cantilevers

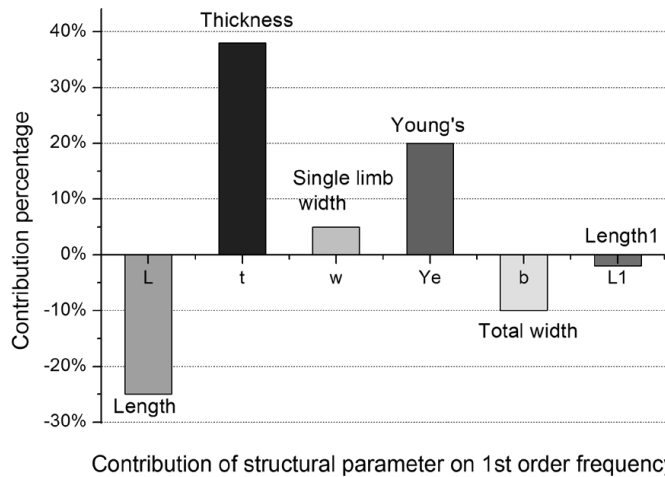


FIG. 11. Contribution percentage of main parameters on the 1st natural frequency.

#### 4. CONCLUSIONS

The finite element method was used to calculate the stiffness and the natural frequencies of two micro-cantilevers commonly used in AFM. The dependence of the behaviour of the rectangular and V-shaped cantilevers on the uncertainty of their dimensional and material parameters was studied. The error limit in this study was set at  $\pm 5\%$  of the nominal value of the parameters which are either the average of the measurement or the one provided by the manufacturer. FE simulations show that the stiffness and the 1st natural frequency of both

cantilevers vary at a much bigger range than the randomness limit introduced in the design parameters. In order to enhance modelling accuracy, the measurement precision of the dimensional parameters must be improved and variations in material properties need to be minimised through strictly controlled fabrication process.

A sensitivity analysis was used to study the influence of design parameters on the 1st natural frequency and the stiffness. It was found that the main factors affecting the accuracy are the length, the thickness, and the Young's modulus, among others. The cantilever length  $L$  has the greatest impact on the natural frequency and the stiffness, and is in a negative correlation. In terms of significance, the thickness of the cantilever  $t$  is the second parameter, and the Young's modulus  $E$  third, affecting the natural frequency with a positive correlation.

For the V-shaped cantilever, the cantilever thickness  $t$  affects the natural frequency most in a positive correlation. This is followed by the length  $L$  in a negative correlation. The effect of the Young's modulus is similar to that of a rectangular cantilever.

In this study, approximation was taken for a simplified fully clamped boundary condition. Moreover, the material is assumed homogeneous and isotropic, which is questionable. For instance, growth lines across the thickness of silicon deposits can be seen in Fig. 5, which may contain oriented textures or defects, resulting in non-homogeneity. All these may contribute to the relatively large difference between the measured and modelled results. This remains to be further studied.

This study provides a clear understanding on the influence of the uncertainty of influential parameters on the behaviour of micro cantilevers used in the AFM technology. It provides useful insights and guidance for the design and calibration of micro cantilevers in AFM.

#### ACKNOWLEDGMENT

Data and information provided by C.T. Gibson of the University of Leeds is high acknowledged.

The research was supported by Sichuan International Research Collaboration Project (2014HH0022).

#### REFERENCES

1. BINNIG G., QUATE C.F., GERBER C., *Atomic force microscope*, Physical Review Letter, **56**, 9, 930–933, 1986.
2. PRATER C.B., BUTT H.J., HANSMA P.K., *Atomic force microscopy*, Nature, **345**, 6, 839–840, 1990.

3. NADER J., KARTHIK L., *A review of atomic force microscopy imaging systems: application to molecular metrology and biological sciences*, *Mechatronics*, **14**, 8, 907–945, 2004.
4. TORTONESE M., *Cantilevers and tips for atomic force microscopy*, Park Scientific Instruments, **16**, 2, 28–33, 1997.
5. SENDEN T.J., DUCKER W.A., *Experimental determination of stiffness in atomic force microscopy*, *Langmuir*, **10**, 4, 1003–1004, 1994.
6. GIBSON C.T., WATSON G.S., MYHRA S., *Determination of the stiffness of probes for force microscopy/spectroscopy*, *Nanotechnology*, **7**, 9, 259–262, 1996.
7. CLEVELAND J.P., MANNE S., BOCEK D., HANSMA P.K., *A nondestructive method for determining the stiffness of cantilevers for scanning force microscopy*, *Review of Science Instruments*, **64**, 2, 403–405, 1993.
8. GIBSON C.T., *Private communication*, Department of Physics and Astronomy, University of Leeds.
9. SADER J.E., LARSON I., MULVANEY P., WHITE L.R., *Method for the calibration of atomic force microscope cantilevers*, *Review of Science Instruments*, **66**, 7, 3789–3798, 1995.
10. GIBSON C.T., SMITH D.A., ROBERTS C.J., *Calibration of silicon atomic force microscope cantilevers*, *Nanotechnology*, **16**, 2, 234–238, 2005.
11. ALBRECHT T.R., AKAMINE S., CARVER T.E., QUATE C.F., *Microfabrication of cantilever styli for the atomic force microscope*, *Journal of Vacuum Science & Technology A*, **8**, 4, 3386–3396, 1990.
12. BUTT H.J. *et al.*, *Scan speed limit in atomic force microscopy*, *Journal of Microscopy*, **169**, 1, 75–84, 1993.
13. CLIFFORD C.A., SEAH M.P., *The determination of atomic force microscope cantilever stiffness via dimensional methods for nanomechanical analysis*, *Nanotechnology*, **16**, 9, 1666–1880, 2005.
14. SADER J.E., *Parallel beam approximation for V-shaped atomic force microscope cantilevers*, *Review of Science Instruments*, **66**, 9, 4583–4587, 1995.
15. COOK R.D., *Finite Element Modelling for Stress Analysis*, John Wiley & Sons Inc Press, 1995, ISBN 0-471-10774-3.
16. Olympus Optical Corporation, Tokyo, Japan.
17. MORRIS V.J., KIRBY A.R., GUNNING A.P., *Atomic Force Microscopy for Biologists*, Imperial College Press, 1999, ISBN 1-86094-199-0.
18. CHEN G.Y., WARMACK R.J., THUNDAT T., ALLISON D.P., HUANG A., *Resonance response of scanning force microscope cantilevers*, *Review of Scientific Instruments*, **65**, 8, 2532–2537, 1994.
19. ASHBY M.F., *Materials selection in mechanical design*, Cambridge University Press, 2005, ISBN 0-7506-4357-9.
20. BARBATO M., CONTE J.P., *Finite element response sensitivity analysis: a comparison between force-based and displacement-based frame element models*, *Computer Methods in Applied Mechanics and Engineering*, **194**, 8, 1479–1512, 2005.
21. WANG S., SUN Y., GALLAGHER R.H., *Sensitivity analysis in shape optimization of continuum structures*, *Computer & Structures*, **20**, 5, 855–867, 1985.

22. MOTTERSHEAD J.E., LINK M., FRISWELL M.I., *The sensitivity method in finite element model updating: A tutorial*, Mechanical Systems and Signal Processing, **25**, 10, 2275–2296, 2011.
23. POLLOCK G.D., NOOR A.K., *Sensitivity analysis of the contact/impact response of composite structures*, Computers & Structures, **61**, 10, 251–269, 1996.
24. PAJOT J.M., MAUTE K., *Analytical sensitivity analysis of geometrically nonlinear structures based on the co-rotational finite element method*, Finite Elements in Analysis and Design, **42**, 6, 900–913, 2006.
25. REEDK.L., ROSE K.A., WHITMORE R.C., *Latin hypercube analysis of parameter sensitivity in a large model of outdoor recreation demand*, Ecological Modelling, **24**, 9, 159–169, 1984.
26. OLSSON A., SANDBERG G., DAHLBLOM O., *On Latin hypercube sampling for structural reliability analysis*, Structural Safety, **25**, 1 47–68, 2003.
27. LIU W., *Design of Experiments*, Tsinghua University Press, 2011.